Electronic Supplementary Material (ESI) for CrystEngComm.

Assembly of three stable POM-based pillar-layer Cu^{I} coordination polymers with visible light driven photocatalytic properties

Xin-Xin Lu,[a] Yu-Hui Luo,[ab] Yu-Shuang Liu,[a] Wen-wen Ma,[a] Yan Xu,[a]and Hong Zhang*[a]

Institute of Polyoxometalate Chemistry, Department of Chemistry, Northeast Normal University, Changchun, Jilin 130024, P. R. China

** E-mail: zhangh@nenu.edu.cn (H. Zhang)*

X-Ray crystallography. Crystallographic diffraction data for **1-2** was recorded on a Bruker Apex CCD diffractometer with graphite monochromatized Mo-*K*α radiation (λ = 0.71073 Å) at 293 k. The structure was solved by Direct Method of SHELXS-97 and refined by full-matrix least-squares techniques using the SHELXL-97 program. All non-hydrogen atoms were refined with anisotropic temperature parameters. All hydrogen atoms on organic ligands were placed in geometrically idealized position as a riding mode. The crystallographic data for **1-2** are summarized in Table S1.

Table S1. Crystal data and structure refinements for **1-2**.

Compounds	**1**	**2**
Formula	$C_{16}H_{16}N_{24}Cu_{12}ClPW_{12}O_{40}$	$C_{16}H_{16}N_{24}Cu_{12}ClPMo_{12}O_{40}$
Fw	4219.63	3164.71
Crystal system	monoclinic	monoclinic
Space group	*C2/m*	*C2/m*
a (Å)	17.507(4)	17.436(2)
b (Å)	14.509(4)	14.520(2)
c (Å)	14.459(14)	14.457(3)
α (deg)	90	90
β (deg)	121.212(7)	121.431(4)
γ (deg)	90	90
V (Å^3)	3140.9(14)	3123.0(9)
Z	2	2
R_{int}	0.1078	0.0557
GOF	1.096	1.051
*R*1, *wR*2 (all data)^a	0.0643, 0.1479	0.0562, 0.1190

$^{a}R_1 = \sum||F_0| - |Fc||/\sum|F_0|$; $wR_2 = \sum[w(F_0^2 - Fc^2)^2]/\sum[w(F_0^2)^2]^{1/2}$.

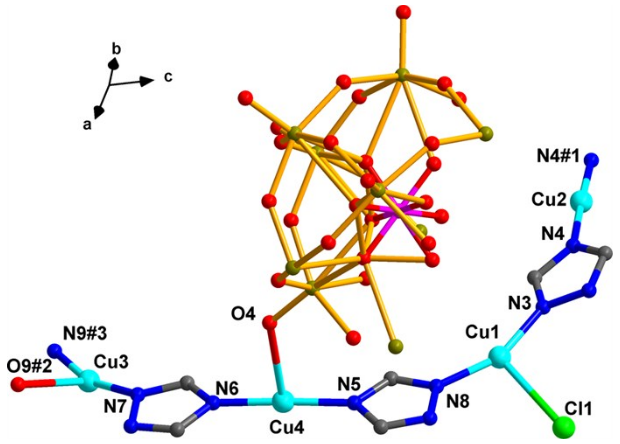

Fig. S1 Coordination environments of Cu ions in compound **1**. Symmetry codes: #1, x, 1-y, z; #2, 1-x, y, -z; #3, x, y, -1+z.

Table S2. Bond valence for compound **1**

bond	bond distance	bond valence	Sum of bond valence
Cu1-N1	1.895	0.362941537	Cu1=0.937
Cu1-N2	1.892	0.365896268	
Cu1-Cl1	2.727	0.208250212	
Cu2-N4	1.868	0.390416742	Cu2=0.781
Cu2-N4	1.868	0.390416742	
Cu3-N7	1.877	0.381034687	Cu3=0.878
Cu3-N3	1.886	0.371878092	
Cu3-O9	2.636	0.124951978	
Cu4-N5	1.868	0.390416742	Cu4=0.867
Cu4-N6	1.857	0.402197985	
Cu4-O4	2.569	0.074878244	

Table S3. Bond valence for compound **2**

bond	bond distance	bond valence	Sum of bond valence
Cu1-N1	1.887	0.332871084	Cu1=0.822
Cu1-N3	1.876	0.342915825	
Cu1-O12	2.601	0.068674428	
Cu2-N4	1.886	0.371878092	Cu2=0.944
Cu2-N6	1.891	0.366886515	
Cu2-Cl1	2.733	0.204900415	
Cu3-N5	1.862	0.396799436	Cu3=0.794
Cu3-N5	1.862	0.396799436	
Cu4-N2	1.873	0.385176328	Cu4=0.845
Cu4-N7	1.872	0.386218753	
Cu4-O4	2.573	0.07407311	

Table S4. Selected bond lengths (Å) and angles (°) of compound **1**.

Cu(1)-N(1)	1.895(13)	N(1) -Cu(1)-Cl(1)	105.2(4)
Cu(1)-N(2)	1.892(11)	N(2) -Cu(1)-Cl(1)	98.6(3)
Cu(1)-Cl(1)	2.727(2)	N(4) -Cu(2)-N(4) #1	176.6(4)
Cu(2)-N(4)	1.868 (14)	N(3)#2-Cu(3)-N(7)	161.9(6)
Cu(2)- N(4)#1	1.868 (14)	N(5)-Cu(4)-N(6)	177.2(9)
Cu(3)-N(3)#2	1.886(13)	Cu(1)-Cl(1)-Cu(1)#3	80.95(8)
Cu(3)-N(7)	1.877(12)	Cu(1)#5-Cl(1)-Cu(1)#3	180.0
Cu(4)-N(5)	1.868 (18)	Cu(1)-Cl(1)-Cu(1)#4	180.0
Cu(3)-N(6)	1.857	Cu(1)-Cl(1)-Cu(1)#5	99.05(8)
N(1) -Cu(1)-N(2)	156.2(5)	Cu(1)#4-Cl(1)-Cu(1)#2	99.05(8)

Symmetry codes: #1, x, -y+1, z; #2, x, y, z-1; #3, x, -y, z; #4, -x+2, -y, -z+2; #5, -x+2, y, -z+2.

Table S5. Selected bond lengths (Å) and angles (°) of compound **2**.

Cu(1)-N(1)	1.887(6)	N(4) -Cu(2)-N(6)	157.3(3)
Cu(1)-N(3)	1.876(7)	N(4) -Cu(2)-Cl(1)	104.62(19)
Cu(2)-N(4)	1.886(7)	N(6) -Cu(2)-Cl(1)	98.06(18)
Cu(2)-N(6)	1.891 (6)	N(5) -Cu(3)-N(5)#1	177.2(4)
Cu(3)- N(5)	1.862 (7)	N(7)#2-Cu(4)-N(2)	175.9(4)
Cu(3)- N(5)#1	1.862 (7)	Cu(2)#3-Cl(1)-Cu(2)	180.0(5)
Cu(4)-N(2)	1.873(9)	Cu(2)#4-Cl(1)-Cu(2)	80.73(4)
Cu(4)-N(7)#2	1.872 (8)	Cu(2)#5-Cl(1)-Cu(2)#4	99.27(4)
Cu(2)-Cl(1)	2.7338(12)	Cu(2)#3-Cl(1)-Cu(2)#5	80.73(4)
N(1) -Cu(1)-N(3)	161.6(3)	Cu(2)#5-Cl(1)-Cu(2)#4	180.0

Symmetry codes: #1, x, -y+1, z; #2, x, y, z-1; #3, -x, -y, -z+1; #4, x, -y, z; #5, -x, y, -z+1.

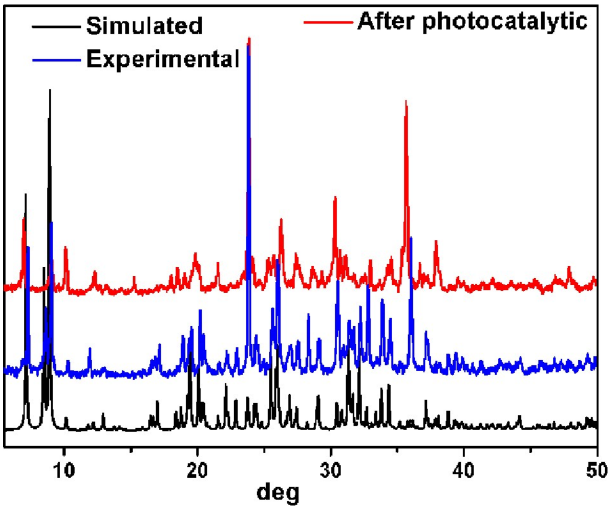

Fig. S2 PXRD patterns of compound **1.**

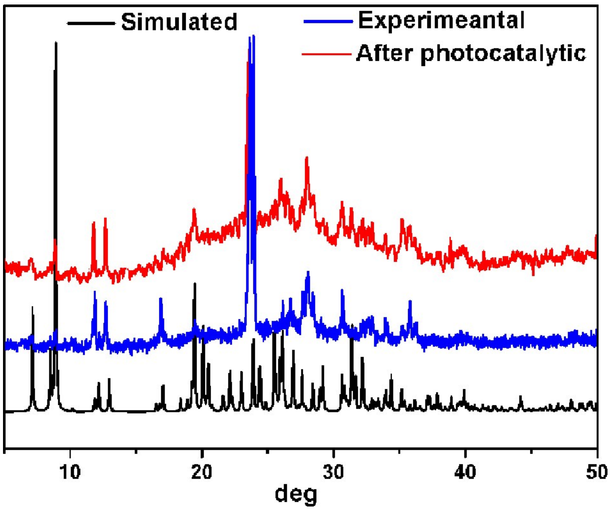

Fig. S3 PXRD patterns of compound **2.**

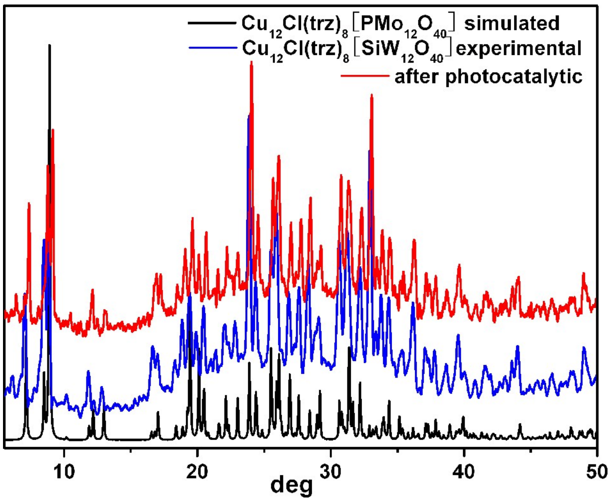

Fig. S4 PXRD patterns of compound **3.**

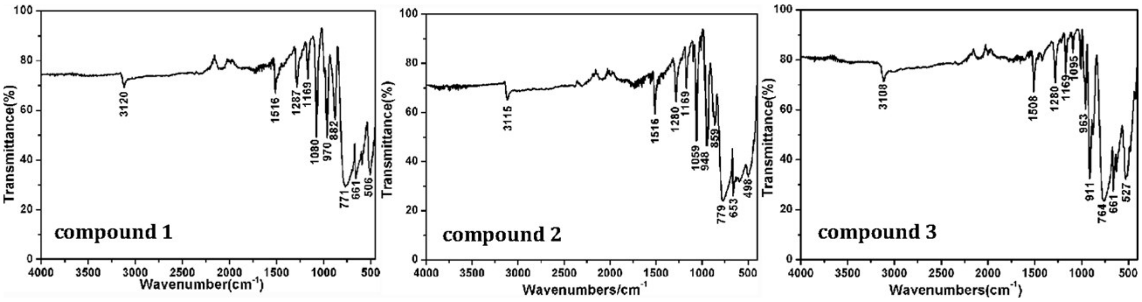

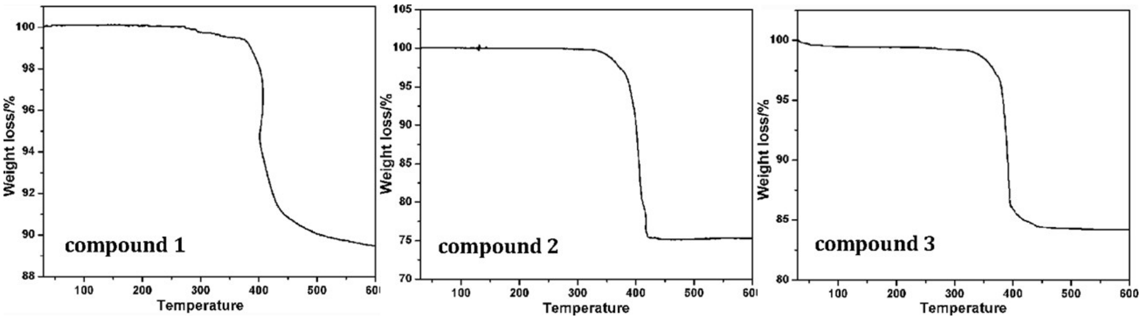

Fig. S5 IR spectra of compounds **1-3.** (above) **Fig. S6** TG curve of compounds **1-3.** (below)

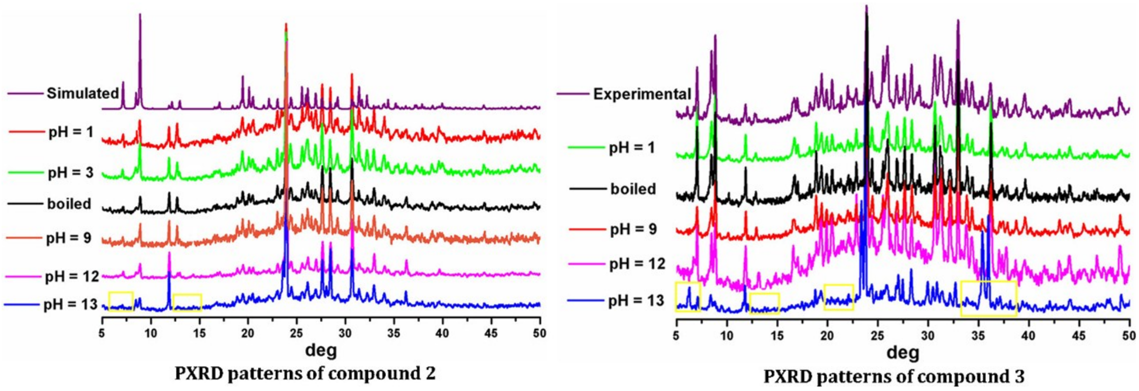

Fig. S7 PXRD patterns for as-synthesized compounds **2-3** and crystals of compounds **2-3** after soaking in different concentrations of HCl, boiling water, or base solution.

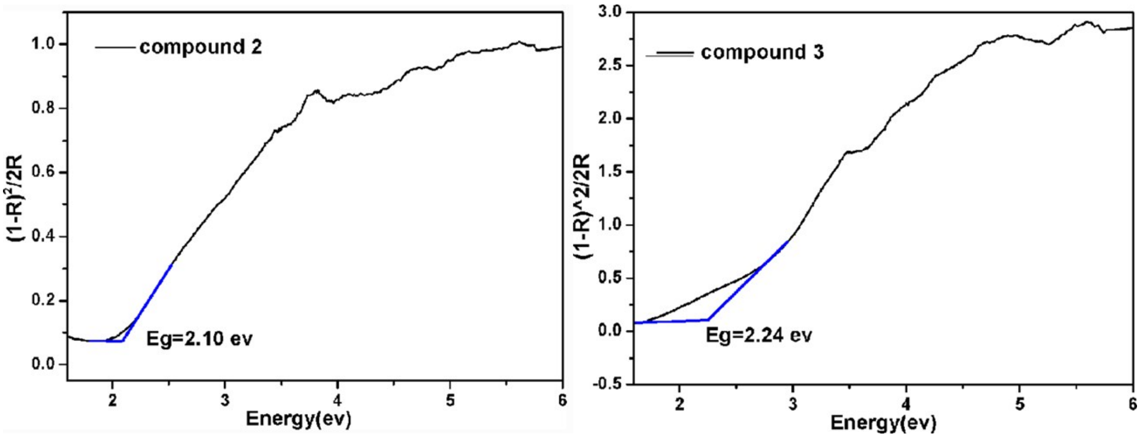

Fig. S8 The $(1-R)^2/2R$ *vs. hv* curve of compound **2-3**.

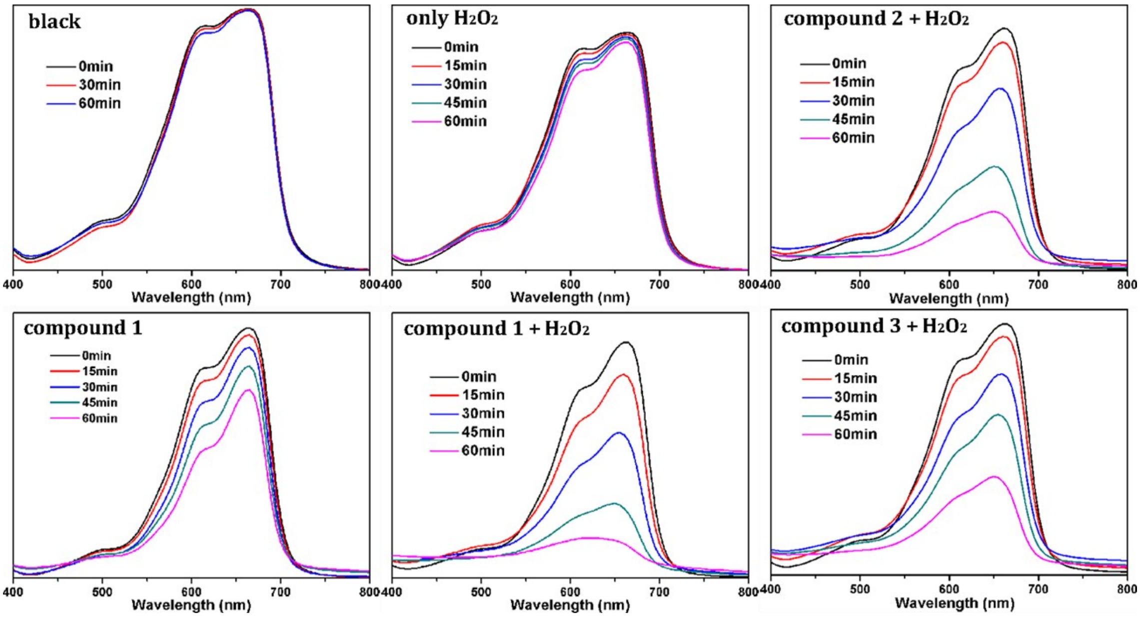

Fig. S9 Photodegradation of MB under visible light irradiation.

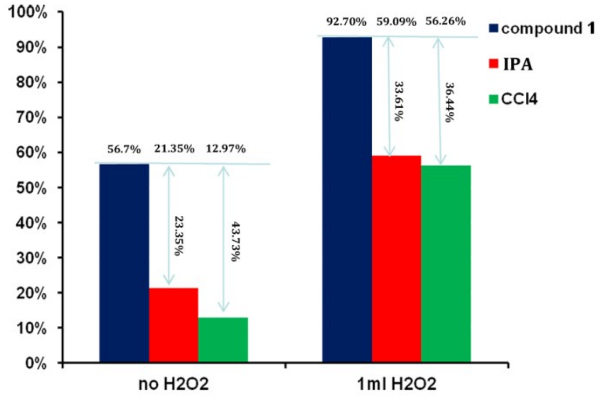

Fig. S10 (a) Photodegradation of MB over catalyst-no H_2O_2 and catalyst-H_2O_2 system under visible light irradiation in the presence of trapping systems (scavenger amount ≈ 45mM，H_2O_2 amount ≈ 95mM).

Photocatalytic Mechanism

The proposed photocatalytic mechanism of **1-3** is shown in Fig. S12. The catalyst is excited by visible light radiation to produce excited state ($e^- + h^+$), which can oxidize H_2O to form ·OH radicals that are oxidants for dye degradation, also can direct oxidize dye molecules into final product $(\text{dye})_{ox}$ (equation (1,2,4)). Besides, when H_2O_2 exists in photocatalytic system, H_2O_2 also captures e^- in this system to generate ·OH to degrade dye molecules (equation (3,4)). Then $(\text{Cat.})_{red}$ is oxidized to Cat. through O_2 in catalytic system (equation (5)).

$\text{Cat.} + \text{vis} \rightarrow (\text{Cat.})_{ox}\ \{\text{POM}(\quad {}^- + h^+)\}$ **(1)**

$(\text{Cat.})_{ox} + \text{dye} \rightarrow (\text{Cat.}) \qquad + (\text{dye})_{ox}$

(2)

$(\text{Cat.})_{ox} + H_2O \rightarrow (\text{Cat.})_{red} \ + \cdot OH + H^+$

$H_2O_2 + e^- \rightarrow \cdot OH + OH^-$ **(3)**

$\cdot OH + \text{dye} \rightarrow (\text{dye})_{ox}$ **(4)**

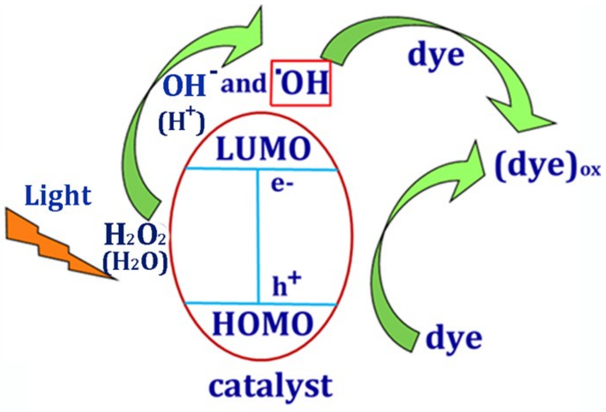

Fig. S11 Schematic diagram of the photocatalytic mechanism of **1-3**.

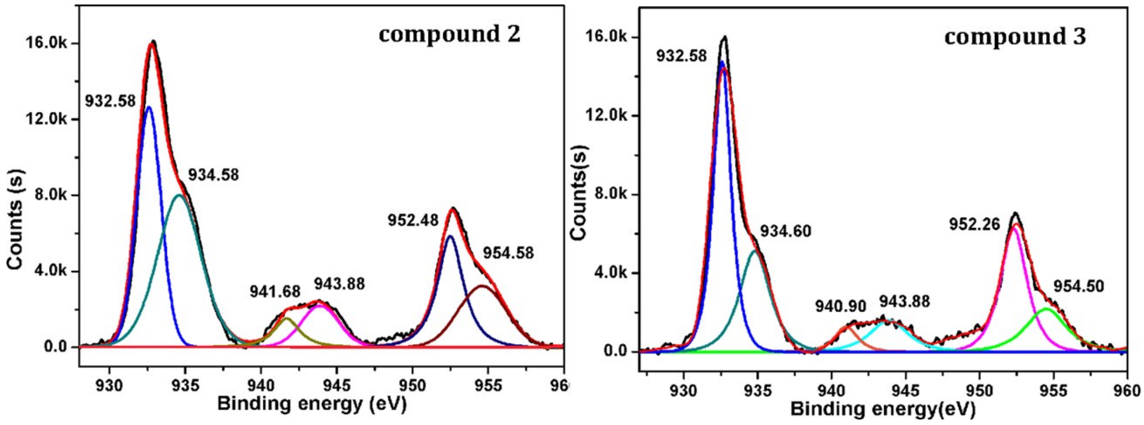

Fig. S12 XPS of Cu in compounds **2-3**.